Exploring the potential of Miller cycle with and without EGR for maximum efficiency and minimum exhaust emissions in a heavy-duty diesel engine

Guan W, Pedrozo VB, Wang X, Zhao H, Ban Z, et al

Abstract

In order to improve the fuel conversion efficiency and meet more stringent exhaust emissions regulations, Miller cycle and exhaust gas recirculation (EGR) have been researched as separate means to reduce carbon dioxide (CO_2) and pollutant emissions from the internal combustion engines. In this paper, an experimental work was carried out to explore the potential benefits of Miller cycle operation via late intake valve closing (LIVC) with and without EGR in a single cylinder heavy-duty (HD) diesel engine equipped with a variable valve actuation (VVA) system. The overall engine-out emissions, fuel conversion efficiency, and estimated urea consumption in the selective catalyst reduction (SCR) aftertreatment were analysed and compared over the World Harmonized Stationary Cycle (WHSC) for different combustion control strategies. Additionally, the potential of Miller cycle with and without EGR based on the “SCR-only” and “SCR + EGR” technical routes to meet the Euro VI nitrogen oxides (NOx) limit of 0.4 g/kWh was assessed at different NOx aftertreatment efficiencies.

When considering the urea consumption in the SCR, the results showed that the introduction of EGR allowed for an engine operation with higher corrected net indicated efficiency ($NIE_{corr.}$) or lower specific total fluid consumption than the baseline cases without EGR due to the relatively lower engine-out NOx emissions. However, the use of EGR adversely affected soot and CO emissions when operating with constant intake pressure (P_{int}) of the baseline case. The application of Miller cycle with and without EGR strategies decreased the net indicated efficiency (NIE) and $NIE_{corr.}$ when operating with the same P_{int} of the baseline operation. The use of higher P_{int} helped to improve upon the NIE and $NIE_{corr.}$ of the Miller cycle cases. The WHSC cycle-averaged analysis showed that different combustion and engine control technologies can be adopted with and without EGR to meet Euro VI NOx limit. A conventional baseline engine operation without EGR would require a high SCR efficiency of 96% in order to curb a cycle-averaged NOx emissions level of 10 g/kWh. Miller cycle operation without EGR achieved the optimum $NIE_{corr.}$ at the cycle-averaged NOx level of 8 g/kWh. When increasing the P_{int}, this strategy enabled an increase of 2.6% in the $NIE_{corr.}$ and reduced the required SCR efficiency to 93.5%, but with a penalty on the NIE of 3.3% when controlling the cycle-averaged NOx level at 6.5 g/kWh. Alternatively, Miller cycle operation with EGR and higher P_{int} allowed for a cycle-averaged NOx levels of 4.0 g/kWh, decreased the total fluid consumption by 8% and minimised the required SCR efficiency to 90%. Therefore, this study has presented promising cost-effective emission control and fuel efficiency technologies that could be suitable for the "SCR-only" and "SCR + EGR" technical routes for the future HD diesel engines.

Keywords

Heavy-duty diesel engine, Miller cycle, EGR, total fluid consumption, exhaust gas temperature, exhaust emissions.

1. Introduction

Growing concerns over the greenhouse gas (GHG) such as CO_2 and increasing stringent emission regulations are driving the development of advanced combustion and engine control technologies. Despite occupy only 4% of the total number of on-road vehicles, the heavy-duty (HD) vehicles account for 18% of the fuel consumption and CO_2 emissions within the transportation sector [1].

HD vehicles, which typically powered by diesel engines, are facing another important concern over high levels of NOx and soot emissions. This is due to the fact that conventional diesel combustion produced a wide range of local in-cylinder gas temperatures and equivalence ratios, which are the two main conditions dominating the formation of NOx and soot emissions [2,3]. These emissions are limited to 0.4 g/kWh and 0.01 g/kWh accordingly in the Euro VI legislation [4]. To meet these low emission targets, significant reduction in these pollutants by in-cylinder combustion technologies and emission control aftertreatment systems is required [5].

Some technical routes have been adopted to meet the emission legislation for HD applications [6]. The first solution that some companies have adopted is the "EGR-only" concept, which relies heavily on EGR utilization requiring up to 40% EGR at full engine load [7,8]. This requires a high performance turbocharging system in order to maintain the in-cylinder air/fuel ratio [9]. The high amount of exhaust gas recirculated back to the engine also increases the demand on the engine cooling systems. Furthermore, advanced high pressure common rail fuel injection system is required in order to avoid excessive soot emissions and poor fuel efficiency. All these required improvements on the original systems would increase the initial cost and the complexity of the engine.

The second widely adopted technical route by manufactures is the "SCR-only" strategy, which can relieve the burden on the engine design while achieving relatively higher fuel conversion efficiency and lower soot emissions. However, the high engine-out NOx emissions requires a very complicated SCR control strategy combined with a high NOx conversion efficiency of more than 95% to comply with the Euro VI NOx limits. The high urea consumption in the SCR system also raises the risk of NH_3 slip, which is limited to less than 10 ppm in the Euro VI regulation [10,11]. Additionally, high SCR conversion efficiency is difficult to maintain at the low engine load operations where the exhaust gas temperature (EGT) is relatively low and probably insufficient to support an efficient SCR system [12].

In comparison with the two aforementioned technical routes, another approach is the combined use of EGR with the SCR strategy. This can simplified the SCR control strategy and lower the EGR requirement, varied from 15% at full load to 30% at lower loads [13,14]. With regard to the engine operational cost, the three technical routes are facing the challenge of the trade-off between exhaust emissions and fuel efficiency. For example, an increase in the fuel conversion efficiency by 1% would lead to higher engine-out NOx emission, increasing from 10 g/kWh to 14 g/kWh [6]. This can increase the total engine operational cost (EOC) due to higher urea consumption in the SCR system [6,15,16]. Likewise, the lower engine-out NOx emissions can be achieved at the expense of a lower fuel efficiency, which can adversely affect the total EOC. Therefore, it is necessary to research alternative in-cylinder combustion and engine control technologies coupled with aftertreatment control strategy in order to achieve fuel efficient and cost-effective solutions [17,18].

Recently, Miller cycle has been shown as an effective engine control technology to reduce in-cylinder NOx formation during the combustion process and is being considered as a mainstream technology to be adopted to HD diesel engines [19]. Firstly, Miller cycle achieved via early or late intake valve closing (IVC) timings can be an effective means for NOx control and therefore potentially minimize the requirement on the EGR rate used. This is because the lower effective compression ratio (ECR) decreases the in-cylinder gas temperatures at the end of the compression stroke and thus lower peak combustion temperature [20–24]. In addition, Miller cycle can effectively decrease the mechanical and thermal loads of a modern turbocharged HD diesel engine by reducing the peak in-cylinder pressure and temperature via a later initiation of compression process. This allows for the application of advanced combustion technologies such as advanced diesel injection timing, higher fuel injection pressure, and higher boost pressure to improve the engine efficiency [25–28]. Moreover, Miller cycle is one of the effective strategies of improving upon exhaust temperature management to facilitate NOx removal by SCR, particularly at light engine load operation. This is primarily attributed to the reduced in-cylinder mass trapped and the delayed combustion process [29–32].

This study aims to explore Miller cycle based cost-effective emission control and fuel efficiency technologies incorporated in the “SCR-only” and “SCR + EGR” technical routes for future HD diesel engines by combining with and/or without EGR. In particular, the current work is the first attempt to experimentally investigate the influence of Miller cycle operating with and without EGR using constant boost pressure and constant lambda of the baseline cases respectively from low to full engine loads, as well as their potential to meet the Euro VI emission regulations over the WHSC test cycle.

The experimental work was carried out on a single-cylinder HD diesel engine. The investigation was conducted at test points within the WHSC test cycle. The results of the different emission control and fuel efficiency technologies were compared with the maximum $NIE_{corr.}$ at a steady-state engine speed of 1250 rpm and engine loads between 25% and 100% of full load. In addition, the cycle-averaged results calculated over the WHSC test cycle were analysed and discussed. Finally, the potential of Miller cycle with EGR and without EGR based on the “SCR + EGR” and “SCR-only” technical routes to meet the Euro VI emission regulation was assessed at different NOx aftertreatment efficiency requirements.

2. Experimental setup

2.1 Test engine

Experiments were carried out on a single cylinder HD diesel engine equipped with a high pressure common rail fuel injection system. The engine was coupled to a Froude Hofmann AG150 eddy current dynamometer in order to absorb the power output. Figure 1 shows the schematic diagram of the experimental setup and Table 1 outlines the specifications of the test engine. The design of the cylinder head with 4-valve and a stepped-lip piston bowl were based on the Yuchai YC6K 6-cylinder engine, while the bottom end/short block was AVL-designed with two counter-rotating balance shafts.

An AVL 515 sliding vanes supercharger was used to provide the boosted intake air with closed loop control. The intake and exhaust surge tanks were installed to damp out the strong pressure fluctuations. Two piezo-resistive pressure transducers were used to measure the instantaneous intake and exhaust manifold pressures. The intake manifold pressure was fine adjusted by an intake throttle valve located upstream of the intake surge tank while the exhaust back pressure was independently controlled through a butterfly valve located downstream of the exhaust surge tank. The intake mass flow rate was measured by an Endress+Hauser Proline t-mass 65F thermal mass flow meter. High-pressure loop cooled external EGR was introduced into the engine upstream of the intake surge tank using a pulse width modulation-controlled EGR valve and the pressure differential between the intake and exhaust manifolds.

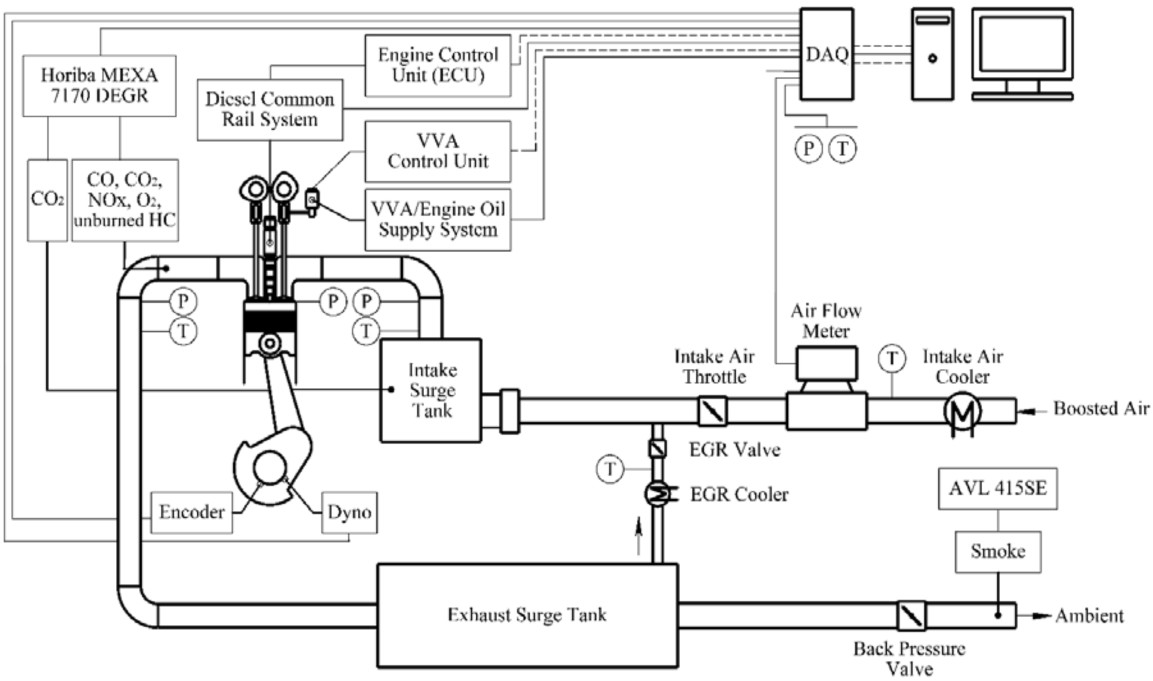

Figure 1. Layout of the engine experimental setup.

Table 1. Specifications of the test engine.

Displaced Volume	2026 cm^3
Stroke	155 mm
Bore	129 mm
Connecting Rod Length	256 mm
Geometric Compression Ratio	16.8
Number of Valves	4
Piston Type	Stepped-lip bowl
Diesel Injection System	Bosch common rail
Nozzle design	8 holes, 0.176 mm hole diameter, included spray angle of 150°
Maximum fuel injection pressure	2200 bar
Maximum in-cylinder pressure	180 bar

Water cooled heat exchangers were used to control the temperatures of the boosted intake air and external EGR as well as engine coolant and lubrication oil, which were supplied externally by separate electric motors.

A dedicated engine control unit (ECU) was used to control the fuel injection parameters such as the injection pressure, start of injection (SOI), and the number of injection pulses (up to three injections per cycle). During the experiments, the diesel fuel was injected into the engine by a high-pressure solenoid injector through a high pressure pump and a common rail with a maximum fuel pressure of 2200 bar. Two Endress+Hauser Promass 83A Coriolis flow meters were used to measure the fuel consumption, which was determined by measuring the total fuel supplied to and from the high pressure pump and diesel injector. The specifications of measurement equipment can be found in Appendix A.

2.2 Variable valve actuation system

A prototype hydraulic lost-motion VVA system was installed on the intake camshaft. On the valve side of the rocker arm, a collapsing tappet was incorporated to allow for the adjustment of the IVC timing and therefore enable Miller cycle operation [33]. The intake valve opening (IVO) and IVC timings of the baseline case were set at 367 and -178 crank angle degrees (CAD) after top dead centre (ATDC), respectively. The maximum intake valve lift event was 14mm. All valve events in this study were considered at 1 mm valve lift. Figure 2 shows the intake and exhaust valve profiles for the baseline as well as the late IVC (LIVC) strategy.

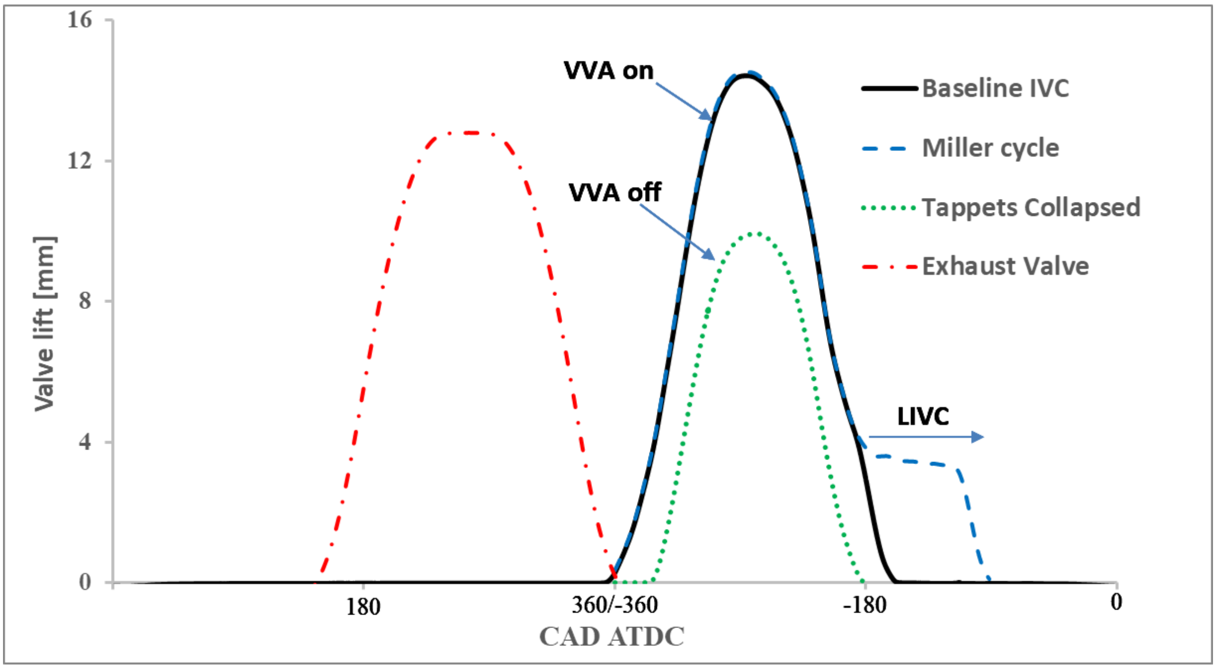

Figure 2. Engine fixed exhaust and variable intake valve lift profiles.

2.3 Exhaust emissions measurement

Gaseous emissions such as NOx, carbon monoxide (CO), CO_2, unburnt hydrocarbon (HC), and oxygen (O_2) were measured by a Horiba MEXA-7170 DEGR emission analyser. A high-pressure sampling module and a heated line were used between the exhaust sampling point and the emission analyser to allow for high-pressure sampling and avoid water condensation. In this study, the EGR rate was defined as the ratio of the measured CO_2 concentration in the intake surge tank ($(CO_2\%)_{intake}$) to the CO_2 concentration in the exhaust manifold ($(CO_2\%)_{exhaust}$) as

$$EGR\ rate\ = \frac{(CO_2\%)_{intake}}{(CO_2\%)_{exhaust}} * 100\% \tag{1}$$

An AVL 415SE Smoke Meter was used to measure the concentration of the black carbon containing soot downstream of the exhaust back pressure valve. The measurement was taken in filter smoke number (FSN) basis, and thereafter was converted to mg/m^3 [34]. All measured exhaust gas components were converted from parts per million (ppm) to net indicated specific gas emissions (in g/kWh) according to the methodology described in the agreement of Regulation number 49 for the European Union [35].

2.4 Data acquisition and analysis

The instantaneous in-cylinder pressure was measured by a Kistler 6125C piezo-electric pressure transducer with a sampling revolution of 0.5 CAD. The measured in-cylinder pressure data was recorded through an AVL FI Piezo charge amplifier. Two National Instruments data acquisition (DAQ) cards were used to acquire the signals from the measurement device. The high speed DAQ card captured high frequency signals such as crank angle resolved data while the low speed DAQ card acquired the low frequency signals of the engine operation. An in-house developed transient combustion analysis software was used to display the captured data from DAQ as well as the processed important engine parameters in real-time.

The crank angle based in-cylinder pressure traces were averaged over 200 consecutive engine cycles for each test point and used to calculate the IMEP and apparent Heat Release Rate (HRR). According to [36], the apparent HRR was calculated as

$$HRR = \frac{\gamma}{(\gamma-1)}\ p\ \frac{dV}{d\theta} + \frac{1}{(\gamma-1)}\ V\ \frac{dp}{d\theta} \tag{2}$$

where γ is defined as the ratio of specific heats, which was assumed constant at 1.33 throughout the engine cycle [37]; V and p are the in-cylinder volume and pressure, respectively; θ is the crank angle.

The pressure rise rate (PRR) was determined by the average value of the maximum pressure variations of one-hundred in-cylinder pressure cycles. The in-cylinder combustion stability was monitored by the coefficient of variation of the IMEP (COV_IMEP) over the sampled cycles. The mass fraction burnt (MFB) was defined by the ratio of the integral of the HRR and the maximum cumulative heat release. Combustion phasing (CA50) was determined by the crank angle of 50% MFB. Combustion duration was represented by the period of time between the crank angles of 10% (CA10) and 90% (CA90) MFB. Ignition delay was defined as the period of time between the main SOI and the start of combustion (SOC), denoted as 0.3% MFB point of the average cycle.

2.5 The definition of the corrected net indicated efficiency

As the urea consumption in the SCR system depends on the operating conditions as well as engine-out NOx emissions, reductions in the levels of engine-out NOx can help minimise the urea flow rate. Therefore, the corrected net indicated efficiency ($NIE_{corr.}$) is used in this study in order to take into account both the measured diesel flow rate ($\dot{m}_{diesel}$) and the aqueous urea solution consumption in an SCR system ($\dot{m}_{urea}$). This allowed for a cost-benefit analysis of the total cost of the different combustion control strategies. The prices of diesel fuel and urea vary in countries and regions and for simplicity they are assumed to be the same in this study [17,38]. According to [17,39,40], the urea consumption in the SCR system can be estimated as 1% of the diesel equivalent fuel flow per g/kWh of NOx reduction necessary to meet the Euro VI limit (NOx_{EuroVI}) of 0.4 g/kWh.

$$\dot{m}_{urea} = 0.01\,(NOx_{Engine\text{-}out} - NOx_{EuroVI})\,\dot{m}_{diesel} \tag{3}$$

The total fluid consumption ($\dot{m}_{total}$) can then be calculated by summing the measured diesel flow rate and the estimated urea flow rate,

$$\dot{m}_{total} = \dot{m}_{urea} + \dot{m}_{diesel} \tag{4}$$

from which the $NIE_{corr.}$ is determined by

$$\mathrm{NIE}_{corr.} = \frac{P_i}{\dot{\mathrm{m}}_{total}\ \mathrm{LHV}_{diesel}} \tag{5}$$

where P_i is the net indicated power and the LHV_{diesel} is the diesel lower heating value of 42.9 MJ/kg. It is noted that in the calculation of the $NIE_{corr.}$ the power used to inject urea is not included and could be included if such data can be available.

3. Methodology

3.1Test conditions

In this study, the effects of Miller cycle combined with different combustion control technologies on engine performance, exhaust emissions, and total engine operational cost were evaluated over the WHSC test cycle, which is a legislated test cycle adopted in the Euro VI emission standard.

Figure 3 shows the location of the WHSC tests points over a HD diesel engine operation map. There are 13 modes in the WHSC test cycle (red circles), which consist of five speeds (25%, 35%, 45%, 55%, and 75%, which are abbreviated as A, B, C, D, and E, respectively) and four engine loads (25%, 50%, 70%, and 100%), as well as two idle modes at the beginning and the end of test cycle. The size of the circle represents the weighting factor. A bigger size indicates a higher relative weighting of the engine operation conditions over the WHSC cycle.

Table 2 summarises the engine operating conditions for the different combustion control strategies investigated between 25% and 100% of full engine loads. The intake pressure (P_{int}) set point of the baseline operation was taken from a Euro V compliant multi-cylinder HD diesel engine of the same cylinder design as the single cylinder engine. The boosted air was supplied by an external boosting system instead of a turbocharger. The exhaust pressures were adjusted to provide a constant pressure differential of 0.10 bar above the intake pressure, in order to realize the required EGR rate and to achieve a fair comparison with equivalent pumping work. Constant lambda and constant P_{int} analyses were carried out on the Miller cycle operation (using the respective set points from the baseline engine operation) to help evaluate the potential of the technology.

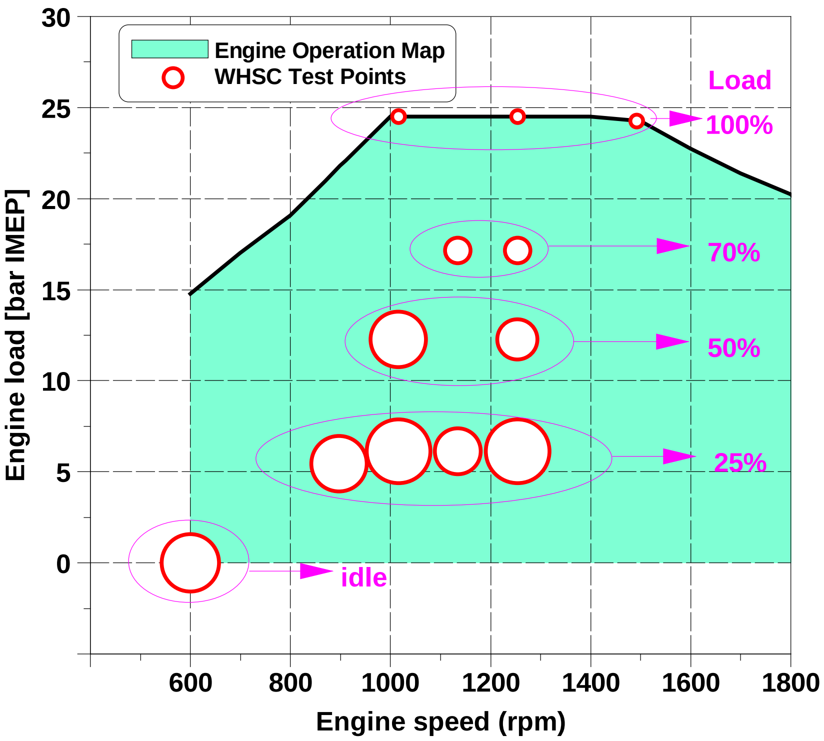

Figure 3. The WHSC operation conditions over an estimated HD diesel engine speed-load map.

With regard to the operations with EGR, the EGR rate was kept constant at a given load, regardless of the combustion control strategy used. An EGR rate of 15% was used between 25% and 70% engine loads, and was decreased to 8% at 100% engine load. The moderate EGR rates were used in this study to avoid the combustion instability, excessive smoke, poor fuel efficiency, as well as to minimise the demand on the boosting system when operating the engine with Miller cycle and EGR. These were also the reasons for the relatively earlier IVC timings used in the cases with EGR when compared to a Miller cycle operation without EGR. The IVC timings of EGR cases were varied from -100 to -130 CAD ATDC and they were from -92 to -120 CAD ATDC for cases without EGR as the engine load increased.

Table 2. Test conditions for baseline and Miller cycle with and without EGR from low to full engine loads.

Engine speed	Engine load	Rail Pressure	EGR	Exhaust pressure	Baseline operation		Miller cycle operation			
					Intake pressure	IVC	Intake pressure		IVC	
							Constant P_{int}	Constant lambda	Without EGR	With EGR
rpm	% of full load	bar	%	bar	bar	CAD ATDC	bar	bar	CAD ATDC	CAD ATDC

897	25	900	0 and 15	0.10 bar higher than the intake pressure	1.20	-178	1.20	1.63	-92	-100
1016	25	1000	0 and 15		1.25	-178	1.25	1.74	-92	-100
	50	1300	0 and 15		1.48	-178	1.48	2.08	-100	-110
	100	1800	0 and 8		2.80	-178	2.80	2.90	-120	-130
1135	25	1000	0 and 15		1.33	-178	1.33	1.95	-92	-100
	70	1400	0 and 15		2.10	-178	2.10	2.32	-110	-120
1250	25	1150	0 and 15		1.44	-178	1.44	2.10	-92	-100
	50	1400	0 and 15		1.74	-178	1.74	2.35	-100	-110
	70	1500	0 and 15		2.30	-178	2.30	2.70	-110	-120
	100	1800	0 and 8		2.80	-178	2.80	3.00	-120	-130
1492	100	1800	0 and 8		2.90	-178	2.90	3.10	-120	-130

During the experiments, a small pilot injection of 3 mm^3 with a constant dwell time of 1 ms prior to the main injection timing was employed for both 25% and 50% engine load conditions in order to keep the maximum PRR below 30 bar/CAD. The coolant and oil temperatures were kept within 85 ± 2°C. Oil pressure was maintained within 4.0 ± 0.1 bar. The maximum in-cylinder pressure was limited to 180 bar. Stable engine operation was determined by controlling the COV_IMEP below 3%.

3.2 The calculation of the pressure-based ECR

In this study, Miller cycle was realised via a LIVC strategy, where the period of intake valves opening was longer than that of the baseline operation. This caused backflow from cylinder into the intake manifold due to the upward piston motion before the IVC, which decreased the actual in-cylinder mass trapped.

The ECR is a commonly used parameter for indicating the extent of compression and quantifying the effect of LIVC, which was reduced by the delayed initiation of the compression process. One of commonly used ECR definitions is based on the volumetric ratio, which is geometrically calculated as the ratio of the cylinder volume at the specified IVC to the cylinder clearance volume at TDC. The actual compression process, however, does not occur exactly when the intake valve close [41]. Figure 4 shows the illustration of the definition of volume-based and pressure-based ECR at a speed of 1250 rpm and a 25% of full load. The cylinder charge has already been partially compressed before the IVC. This is primarily due to the flow resistance across the intake valves and the gas-momentum-induced compression [42]. As a result, the volume-based geometric ECR is generally lower than the pressure-based ECR, as shown in Figure 5. Therefore, the volume-based geometric ECR is inadequate to explain the experimental results.

In this work, a pressure-based method was applied in order to more accurately characterize the actual in-cylinder compression process. The effective IVC volume was taken as the volume corresponding to the intersection point by extrapolating the polytropic compression process curve linearly down to intersect the average intake manifold air pressure (MAP). The pressure-based ECR is then defined as the ratio of the volume at effective IVC to the clearance volume at TDC [43,44].

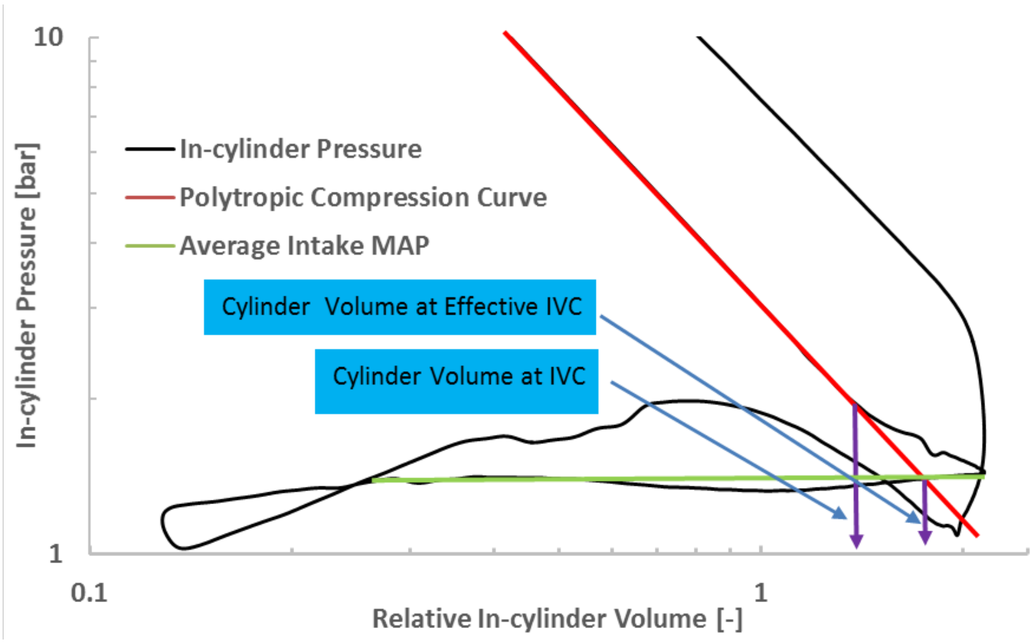

Figure 4. The illustration of volume-based and pressure-based methods for ECR calculation at 1250 rpm and 25% of full load.

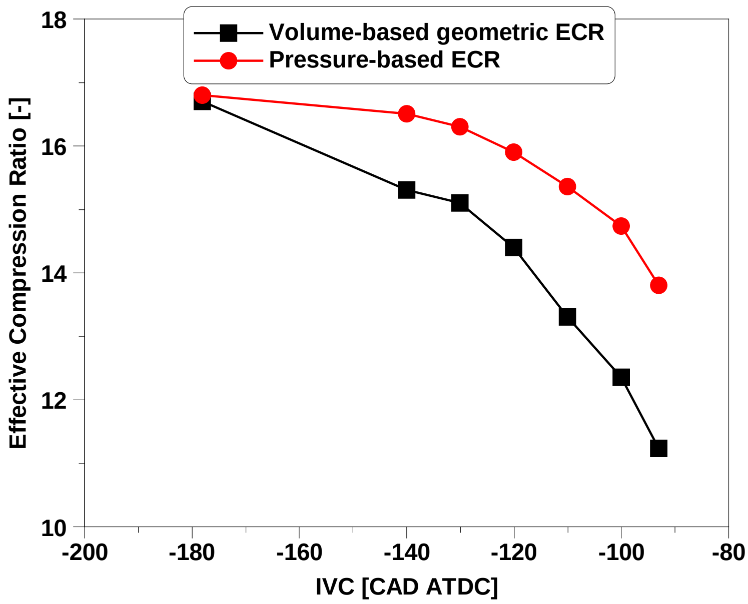

Figure 5. The volume-based and pressure-based ECR as a function of the IVC at 1250 rpm and 25% of full load.

4. Results and discussions

4.1 Miller cycle operation with and without EGR

In this subsection, Miller cycle operation with and without EGR using constant P_{int} and a constant lambda as those of the baseline cases were investigated in order to analyse the effect of Miller cycle on engine performance, exhaust emissions, and total engine operational cost over the engine loads. The results were analysed and comparisons were made with the baseline operations at 1250 rpm over a range of loads from 25% to 100% of full engine load. Diesel injections were optimised for the maximum $NIE_{corr.}$.

4.1.1 Analysis of the in-cylinder pressure and heat release rate

Figure 6 shows the in-cylinder pressure, HRR, and diesel injector signal for cases attained the maximum $NIE_{corr.}$ at 50% of full engine load. The Miller cycle operation without EGR and with a constant P_{int} of 1.74 bar as the baseline operation was characterised by lower in-cylinder pressure and peak HRR. This was due to the later initiation of the compression process by the LIVC and hence lower in-cylinder compressed pressure and temperature. The use of EGR allowed for a more advanced diesel SOI to achieve the maximum $NIE_{corr.}$ when compared to the cases without EGR. This enabled an earlier SOC, consequently increasing the peak in-cylinder pressures (P_{max}) of the optimum cases. When operating with constant lambda by increasing the intake pressure, Miller cycle with and without EGR achieved relatively higher peak HRR, although a later main SOI than that with constant P_{int}.

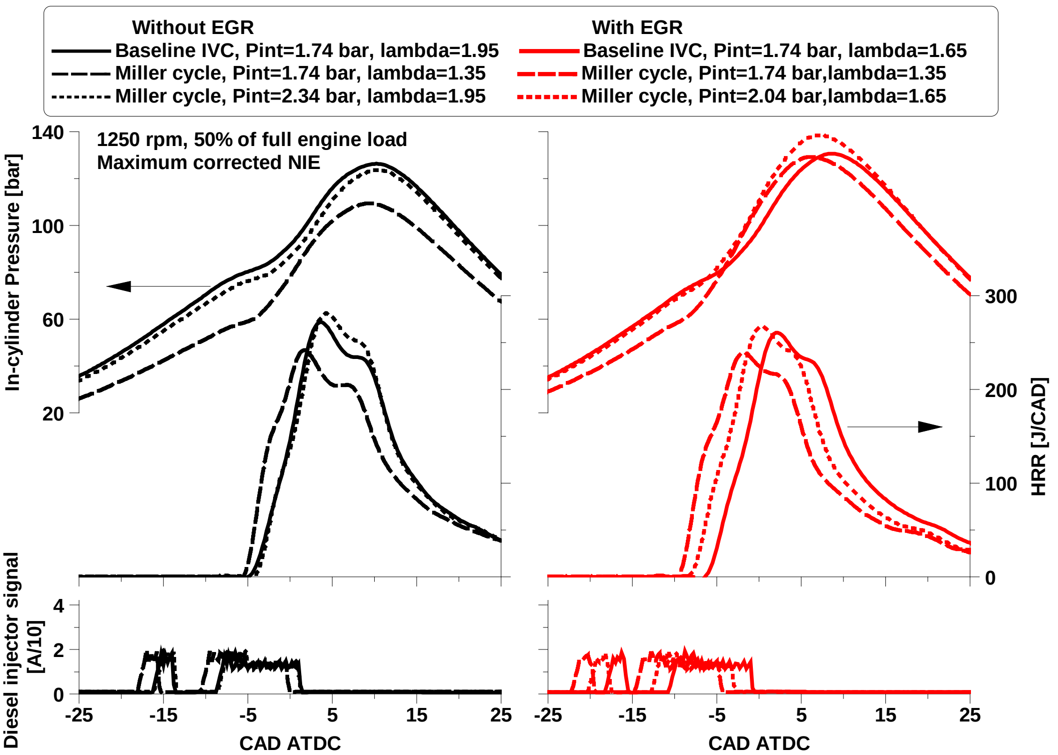

Figure 6. In-cylinder pressure, HRR, and diesel injector signal for the baseline and Miller cycle cases with the maximum $NIE_{corr.}$.

4.1.2 Combustion characteristics

Figure 7 shows the main SOI and the resulting combustion characteristics for the baseline and Miller cycle cases that attained the maximum $NIE_{corr.}$. The Miller cycle with constant P_{int} of the baseline cases allowed for more advanced main SOI, particularly in the cases with EGR. At 100% of full engine load, the optimisation of SOI was constrained by the P_{max} of 180 bar. The Miller cycle and EGR strategies increased the ignition delay in most cases. This was attributed to the lower compression pressures and in-cylinder oxygen availability, as well as the advanced SOI. The PRR was kept below 30 bar/CAD for all cases.

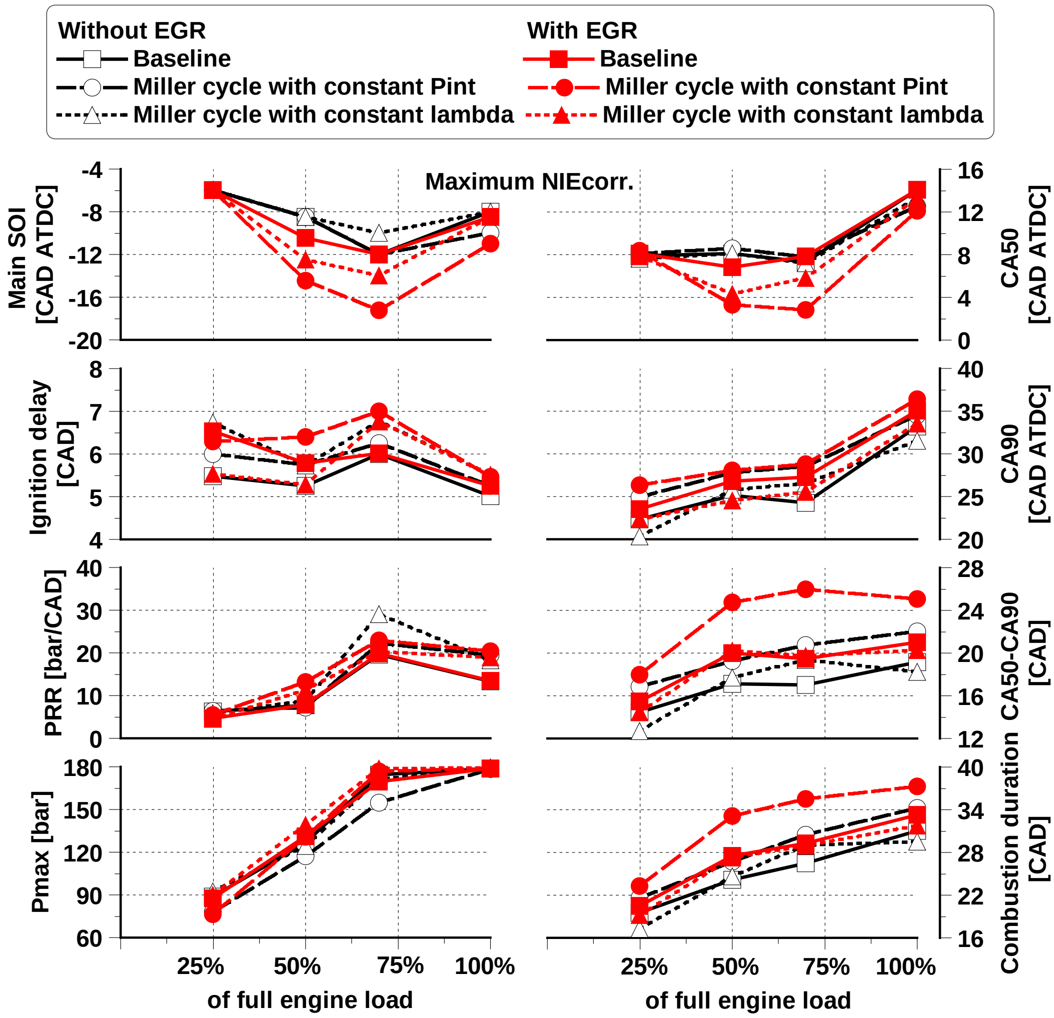

Figure 7. Injection timing and combustion characteristics of the baseline and Miller cycle cases with maximum $NIE_{corr.}$.

The optimum CA50 was initially advanced from low to medium loads likely due to the longer period CA10-CA90 and lower heat transfer losses, and then was delayed at high engine loads attributed to the limit of peak in-cylinder pressure [16]. This trend became more obvious for the cases with EGR. The reduced in-cylinder oxygen availability via the use of Miller cycle and EGR slowed down the rate of heat release, leading to a later CA90 and longer period of CA10-CA90 (e.g. combustion duration). A higher P_{int} improved the in-cylinder oxygen availability and accelerated the combustion process of Miller cycle with and without EGR.

This advanced the CA90 and yielded shorter CA50-CA90 period and combustion duration when operating with a constant lambda.

4.1.3 Engine performance, exhaust emissions, and fuel efficiency

Figure 8 shows the engine performance parameters and net indicated specific emissions for the baseline and Miller cycle cases with and without EGR. Miller cycle with a constant P_{int} decreased the lambda due to a reduction in the in-cylinder mass trapped, particularly with EGR. This was the primary reason for an increase in EGT. However, the “EGR-only” strategy showed little impact on the EGT due to the replacement of air with the recirculated exhaust gas and lower combustion temperatures [24].

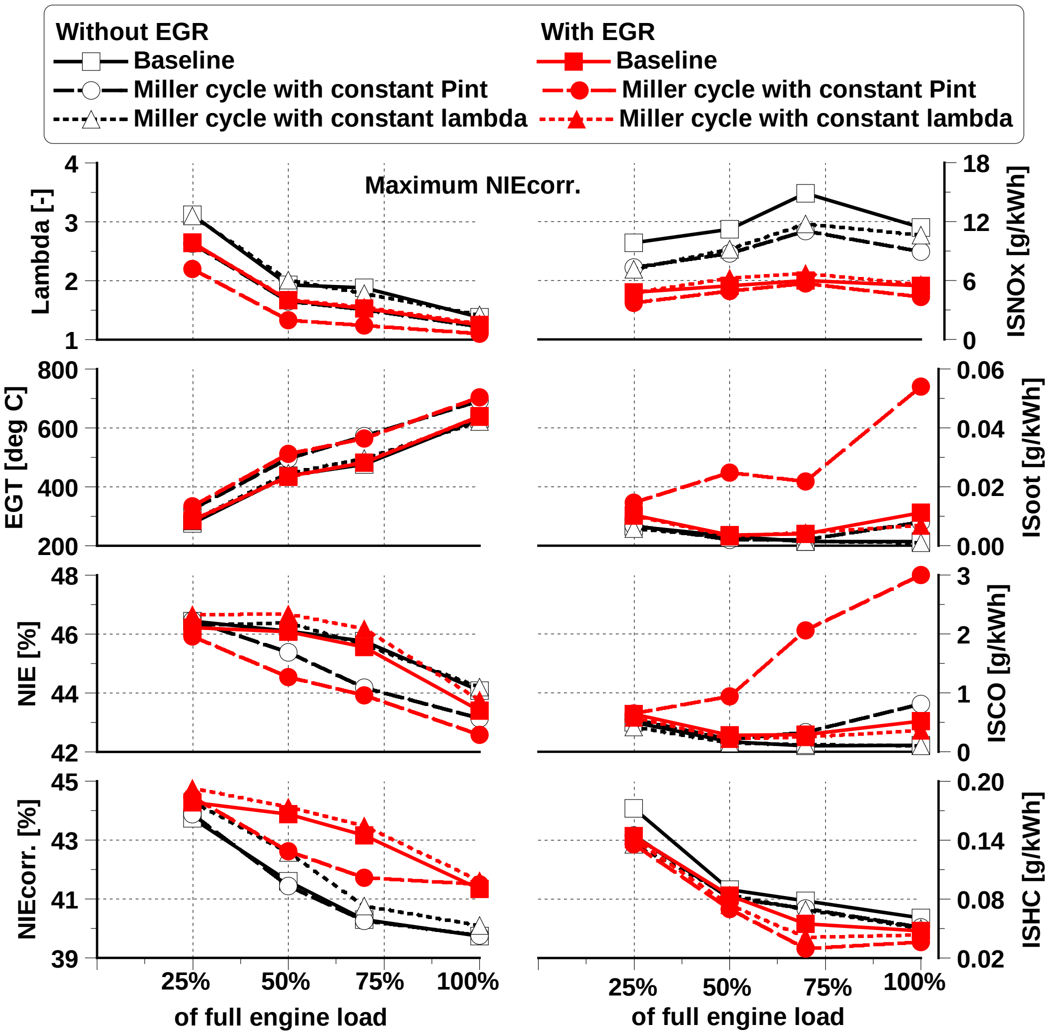

Figure 8. Engine performance, emissions, and fuel efficiency of the baseline and Miller cycle cases with the maximum $NIE_{corr.}$.

Compared to the baseline engine operation, Miller cycle with and without EGR decreased the NIE at a constant P_{int}. This was a result of the slower combustion process and longer combustion duration. The reduction in NIE is also associated with an increase in heat loss due to the higher mean in-cylinder gas temperature calculated by a 1-D engine model, as reported in [24,45]. By using a higher P_{int} to improve the in-cylinder oxygen availability, however, the NIE of Miller cycle was improved and was slightly higher than that of the baseline operation when operating with a constant lambda.

When considering the urea consumption in the SCR system, the total engine operational cost is related to the $NIE_{corr.}$, which will be determined by the engine-out NOx emissions and the fuel conversion efficiency. As shown in the bottom left of Figure 8, the engine operations with EGR achieved higher maximum $NIE_{corr.}$ than those cases without EGR over the sweep of engine loads as a result of the lower NOx emissions. When operating without EGR, the maximum $NIE_{corr.}$ of Miller cycle with constant P_{int} was comparable to that of the baseline. When operating with EGR, Miller cycle strategy significantly reduced the maximum $NIE_{corr.}$. However, by increasing P_{int} and keeping the lambda constant helped to improve the trade-off between NOx emissions and NIE, increasing the $NIE_{corr.}$ of the Miller cycle strategy.

It can be also seen from Figure 8 the engine-out emissions of NOx, soot, unburned HC, and CO. The NOx emissions were increased between 25% and 70% of full engine load but then decreased at 100% of full engine load. This was likely due to the increased combustion temperature from 25% to 70% of full engine load. The NOx reduction at full engine load was associated with the significantly lower lambda value and the relatively retarded CA50. The use of EGR was more effective in minimizing engine-out NOx emissions than Miller cycle in all cases. The "Miller cycle + EGR" strategy with constant P_{int} achieved low NOx levels but yielded excessive smoke, particularly at high engine loads. Soot emissions were reduced when operating with the same lambda of the baseline cases and were maintained below the Euro VI limit of 0.01 g/kWh at 50% and 70% of full engine load. Therefore, the use of high boost pressures is a key enabler for achieving simultaneous low NOx and soot emissions when operating Miller cycle and EGR, especially at high engine loads.

The observed trend of CO emissions was similar to that of soot emissions. This was mainly because the in-cylinder oxygen concentration played an important role on the CO and soot formations. Miller cycle and EGR strategies showed little impact on CO emissions except when they were combined. The use of a higher P_{int} between medium and full engine loads helped to curb CO emissions from the Miller cycle operating with EGR. Finally, Figure 8 revealed that all advanced combustion control strategies decreased HC emissions compared to the baseline cases. Overall, the lowest levels of HC emissions were achieved by the "Miller cycle + EGR" strategy with constant P_{int}. This could be linked to the use of more advanced diesel injections and higher average in-cylinder gas temperature at lower lambda [28].

4.2 Analysis of Miller cycle operation with and without EGR over the WHSC test cycle

The purpose of this subsection is to analyse and compare the cycle-averaged performance, emissions, and total engine operational cost of different combustion control strategies over the WHSC test cycle. The diesel SOI was delayed at each combustion control strategy in order to obtain the different cycle-averaged NOx emissions.

4.2.1 Cycle-averaged engine exhaust emissions as a function of engine-out NOx emissions

Figure 9 shows the exhaust emissions as a function of different cycle-averaged NOx emissions over the WHSC test cycle for the baseline and Miller cycle operations with and without EGR. The diesel SOI was varied to achieve different engine-out NOx emissions in order to obtain the required cycle-average NOx levels for all strategies investigated.

The cycle-averaged soot emissions of all combustion control strategies increased with the reduction in cycle-averaged NOx emissions. The baseline operation without EGR showed little impact on soot emissions when the NOx emissions were controlled at approximately 10 g/kWh or higher. Further reduction in the NOx emissions by delaying the SOI resulted in higher soot emissions. Miller cycle operation without EGR produced less soot emissions than the baseline cases at the NOx level of 8 g/kWh. This was a result of a more advanced diesel injection, which helped improve the air-fuel mixing. However, the soot emissions were increased linearly as the cycle-averaged NOx emissions decreased to below 6.5 g/kWh.

EGR is required to achieve a cycle-averaged NOx emission lower than 6 g/kWh. The results indicated that the use of EGR was effective in reducing NOx emissions while producing slightly higher soot emissions. However, the combination of Miller cycle and EGR at a constant P_{int} produced excessive soot emissions due to the lower lambda at such conditions. This was overcome by increasing intake pressure and was maintained below Euro VI soot limits, as denoted with a red dash line in Figure 9. As a result, simultaneous low levels of soot and NOx emissions were obtained when the engine was operated with the same lambda as the baseline case with EGR.

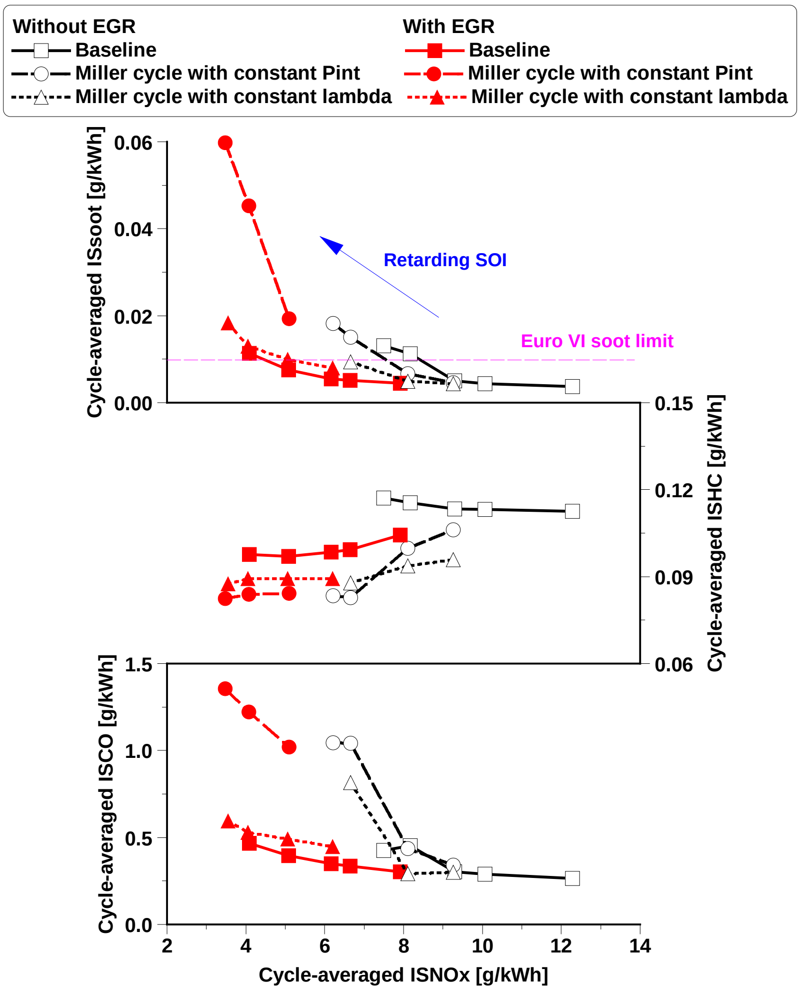

Figure 9. Cycle-averaged exhaust emissions for baseline and Miller cycle cases over the WHSC test cycle.

The data in Figure 9 also shows the cycle-averaged CO emissions, which increased with the reduction in cycle-averaged NOx emissions. Similar to the impact on soot emissions, the SOI in the baseline operations had little impact on the CO emissions. However, the use of late SOI in the Miller cycle operation with a constant P_{int} increased the CO emissions, particularly when using EGR. This drawback was overcome when operating with a higher P_{int}. Different from the soot and CO emissions, HC emissions decreased with a reduction in NOx emissions for all advanced combustion control strategies. These improvements were relatively higher in the Miller cycle cases. Overall, the cycle-averaged CO and HC emissions of all cases were maintained within the Euro VI limits. It should be also noted that CO and HC emissions are not the primary issues in conventional diesel engines. This is due to the fact that HD diesel engines are equipped with a diesel oxidation catalyst (DOC) which can effectively reduce CO and unburnt HC emissions from the engine exhaust gases when the exhaust temperatures were held between 200 and 450°C [46].

4.2.2 Analysis of cycle-averaged performance and potential of different technical routes

This section is focused on the analysis and estimation of the different technical routes in terms of the total engine operational cost and the economic effect by taking into account both fuel consumption and the usage of urea. Figure 10 depicts the cycle-averaged performance as a function of various cycle-averaged NOx emissions for all combustion control strategies. The EGT increased with the reduction in the cycle-averaged NOx emissions. This was due to the use of Miller cycle, EGR, and late SOI for NOx control, which decreased the in-cylinder air mass trapped and/or delayed the combustion process. The highest increase in EGT of approximately 140℃ was achieved by the "Miller cycle-only" strategy. The addition of EGR in the Miller cycle operation had little impact on the EGT, despite the lower lambda.

In addition, all combustion control strategies yielded lower NIE when reducing the cycle-averaged NOx emissions. The baseline operations achieved lower NOx emissions via a retarded SOI, reducing the NOx emissions by 39% with a penalty of 6% in NIE. Compared to the baseline without EGR, the "Miller cycle-only" strategy achieved a reduction in NOx emissions of 49% with the same NIE penalty of 6%. The NIE penalty could be reduced to 3% while preserving the NOx reduction benefit by increasing the P_{int} and maintaining the same lambda of the baseline engine operation. The "EGR-only" strategy reduced the NOx emissions by 67% with a NIE penalty of 2.7%. Alternatively, the "Miller cycle + EGR" strategy with the same lambda as the baseline cases with EGR reduced NOx emissions by up to 71%. This was achieved with the same NIE penalty of 2.7% measured in the "EGR-only" strategy.

Furthermore, the SCR conversion efficiency was used to calculate the urea consumption and the $NIE_{corr.}$ of the engine operation, in order to fully evaluate the potential of these different combustion control strategies to meet different engine-out NOx levels over the WHSC test cycle. It can be seen from Figure 10 the cycle-averaged urea consumption in the SCR system as a function of cycle-averaged NOx emissions. The advanced combustion control strategies helped decrease the urea consumption via lower engine-out NOx emissions. This could minimise the cycle-averaged total fluid consumption and therefore increased the $NIE_{corr.}$. The "Miller cycle + EGR" strategy with a constant lambda attained the highest $NIE_{corr.}$ over the WHSC, increasing the cycle-averaged engine efficiency by up to 8% in comparison with the baseline without EGR.

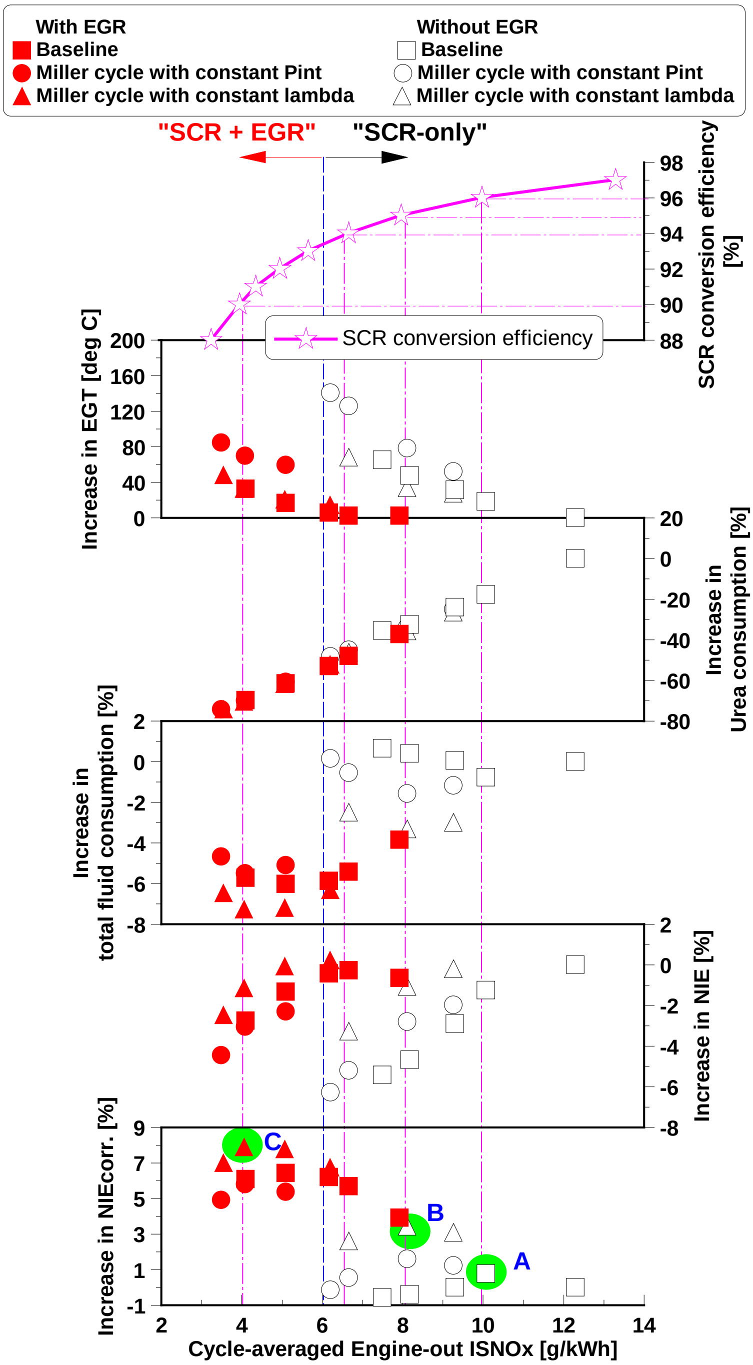

Figure 10. Potential of the proposed "SCR-only" and "SCR + EGR" technical routes to meet the Euro VI NOx limit (0.4 g/kWh) over the WHSC test cycle. A) Optimum baseline engine operation without EGR; B) Optimum "Miller cycle-only" strategy with constant lambda; C) Optimum "Miller cycle + EGR" strategy with constant lambda.

Finally, Figure 10 demonstrates the potential of different combustion control strategies to meet the Euro VI emission regulations. It should be noted that the proposed "SCR + EGR" and "SCR-only" technical routes represent the combustion control strategy with and without using EGR, respectively. The results demonstrated that the baseline case without EGR was adequate for the cycle-averaged NOx emissions of 10 g/kWh and would require an overall SCR conversion efficiency of 96% at the expense of 1.5% reduction in NIE. In addition, the optimum $NIE_{corr.}$ of the baseline engine operation was achieved at this cycle-averaged NOx level of 10 g/kWh, as denoted by point "A" in the bottom of Figure 10. When the cycle-averaged NOx emissions were required to be lower than 10 g/kWh, the Miller cycle without EGR strategy was preferable when operating with a constant lambda of the baseline case without EGR. This strategy enabled a relatively lower penalty of 3.3% on the NIE and an increase of 2.6% in the $NIE_{corr.}$ at the NOx level of 6.5 g/kWh. Besides, the EGT was increased by 68℃ and the minimum required SCR conversion efficiency was reduced to 93.5%. It should be also noted that the optimum $NIE_{corr.}$ of "Miller cycle-only" strategy was improved up to 3.5% when controlling the NOx level at 8 g/kWh, as denoted by point "B" in Figure 10. Therefore, the "Miller cycle-only" strategy with a constant lambda of the baseline case without EGR was determined as the most effective means for the "SCR-only" technical route, achieving lower engine operational cost, higher EGT, and lower soot emissions when the engine-out NOx emissions were kept between 6 and 10 g/kWh.

When the cycle-averaged NOx emissions were controlled to below 6 g/kWh, however, the "Miller cycle-only" strategy resulted in a penalty of 6.3% on NIE and adversely affected the $NIE_{corr.}$. Therefore, the introduction of EGR was necessary owing to its high NOx reduction capability and relatively lower penalty on the fuel conversion efficiency. Particularly, the "Miller cycle +EGR" strategy with constant P_{int} could decrease the cycle-averaged NOx emissions from 12.3 g/kWh in the baseline operation without EGR to 3.4 g/kWh while increasing upon the $NIE_{corr.}$ by 4.9%, despite a reduction in NIE of approximately 4.6%. Meanwhile, this lower cycle-averaged NOx emissions allowed for a reduction in the minimum required SCR conversion efficiency down to 88%, which can significantly minimize the catalyst volumes and thus can simplify the SCR system [47]. However, this strategy increased the cycle-averaged soot emissions to up to 0.06 g/kWh as a result of the lower lambda, which was significantly higher than the Euro VI limit of 0.01 g/kWh (seen in Figure 9). These results can limit the potential of the "Miller cycle + EGR" strategy for efficient and clean engine operation.

Preferably, a more efficient Miller cycle operation with EGR was achieved by keeping the lambda as much as the baseline operation with EGR via a higher P_{int}. The cycle-averaged soot emissions were significant reduced and were controlled within the Euro VI limit at most cases, except for the cases with cycle-averaged NOx emissions below 4 g/kWh, as shown in Figure 9. Meanwhile, the penalty on the NIE was notably minimized and the $NIE_{corr.}$ was significantly increased while maintaining low levels of NOx emissions. Overall, the “Miller cycle + EGR” strategy with a constant lambda achieved the highest improvement in the $NIE_{corr.}$ of 8% when controlling the cycle-averaged NOx emissions at 4 g/kWh, as denoted by point “C” in Figure 10. This was accompanied with an increase in EGT by 40℃ and a lower minimum required SCR conversion efficiency of 90% when compared to the baseline engine operation without EGR. Therefore, the “Miller cycle + EGR” strategy with a higher P_{int} was identified as the most effective means for the “SCR + EGR” technical route, achieving low engine operational cost while simultaneously enabling low cycle-averaged exhaust emissions.

5. Conclusions

This study investigated the effect of Miller cycle with and without EGR on the combustion characteristics, exhaust emissions, and performance of a HD diesel engine over the WHSC tests cycle. Miller cycle, EGR, and multiple injections were achieved by means of a VVA system, a high-pressure loop cooled EGR, and a common rail fuel injection system, respectively. A comparison was performed between the baseline and Miller cycle operations with and without EGR attained the maximum $NIE_{corr.}$ from low to full engine loads. Experimental analysis of cycle-averaged results of the different combustion control strategies were carried out in order to demonstrate their potential to meet the Euro VI NOx limit. The aim of the research was to explore a cost-effective emission control and fuel efficiency technology based on the “SCR-only” and “SCR + EGR” technical routes for the future HD diesel engines. The primary findings can be summarised as follows:

1. At the optimum efficiency and without taking into account the urea consumption in the SCR system, Miller cycle with and without EGR decreased the NIE at the same intake pressure as the baseline operation. This was due to the decreased cylinder mass trapped, resulting in slower combustion process and a longer combustion duration. By increasing the boost pressure to keep the same lambda as the baseline, the NIE of Miller cycle operation was improved and comparable to that of the baseline operation at all engine loads.
2. When considering the total fluid consumption (e.g. fuel and urea), the baseline engine operation with EGR produced higher $NIE_{corr.}$ attributed to the reduction of urea consumption in SCR systems. This reduced the total fluid consumption but at the expense of higher soot and CO emissions. Particularly, the “Miller cycle + EGR” strategy with

constant lambda achieved the highest NIE and $NIE_{corr.}$ while achieving simultaneous low levels of exhaust emissions from low to full engine loads.

3. The cycle-averaged results over the WHSC test cycle showed that all advanced combustion control strategies enabled a reduction in the cycle-averaged NOx emissions and higher EGT. These improvements were attained at the expense of lower NIE and higher soot and CO emissions. However, a higher $NIE_{corr.}$ could be achieved via lower urea consumption in the SCR system, especially when operating with a higher intake pressure to improve the combustion process.
4. The "Miller cycle-only" strategy with constant intake pressure achieved a reduction in the cycle-averaged NOx emissions by 49% at the expense of a penalty on NIE of 6%. When increasing the intake pressure to maintain the same lambda of the baseline operation without EGR, the "Miller cycle-only" strategy enabled a relatively lower penalty of 3.3% on the NIE and an increase in the $NIE_{corr.}$ of 2.6% at the cycle-averaged NOx level of 6.5 g/kWh. In the meantime, the cycle-averaged EGT was increased by 68℃, which was associated with the decrease in the cylinder mass and thus a lower total heat capacity.
5. The "Miller cycle + EGR" strategy with constant intake pressure could decreased the cycled-average NOx emissions from 12.3 g/kWh in the baseline operation without EGR to 3.4 g/kWh, but adversely affected soot emissions and NIE. The use of a higher intake pressure to maintain the same lambda of the baseline operation with EGR enabled a "Miller cycle + EGR" strategy achieving the highest improvement of approximately 8% in the $NIE_{corr.}$ while elevating the EGT by 40℃ and controlling the NOx levels at 4 g/kWh. Meanwhile, the highly boosted strategy helped increase the NIE and curb soot emissions due to improved oxygen availability and thus the combustion process.
6. Overall, the "Miller cycle-only" and "Miller cycle+ EGR" strategies with the same lambda as the baseline operations were identified as the most effective emission control and fuel efficiency technologies for the "SCR-only" and "SCR + EGR" technical routes accordingly. Moreover, the minimum required SCR conversion efficiency was reduced from 96% in the baseline engine operation to 93.5% in the "Miller cycle-only" strategy and 90% in the "Miller cycle+ EGR" strategy when they were combined with a highly boosted strategy.

6. Future work

From the results presented in this study, it can be seen that the application of Miller cycle required a higher boost pressure to recover the cylinder charge air in order to avoid lower engine efficiency. This increases the requirements on the boosting system, a conventional turbocharging system is likely not able to deliver the required airflow rate. Thus, a more sophisticated boosting system such as a two-stage VGT configuration will be needed to deliver the desired boost pressure, but it largely increases the engine complexity and requires additional cost and may increase the total engine operational cost. Additionally, a highly efficient intake intercooler will be essential to cool down the boosted intake air.

Moreover, the impact of applying Miller cycle on turbocharger and pumping work as well as aftertreatment systems needs to be investigated on a multi-cylinder engine, so that further improvement and better understanding of such technology in real world applications can be assessed.

Definitions/Abbreviations

CA90	Crank Angle of 90% Cumulative Heat Release.
CA50	Crank Angle of 50% Cumulative Heat Release.
CA10	Crank Angle of 10% Cumulative Heat Release.
ATDC	After Firing Top Dead Center.
CAD	Crank Angle Degree.
CO	Carbon Monoxide.
CO_2	Carbon Dioxide.
COV_IMEP	Coefficient of Variation of IMEP.
$(CO_2\%)_{intake}$	CO_2 concentration in the intake manifold.
$(CO_2\%)_{exhaust}$	CO_2 concentration in the exhaust manifold.
DOC	Diesel Oxidation Catalyst.
ECR	Effective Compression Ratio.
ECU	Electronic Control Unit.
EGR	Exhaust Gas Recirculation.
EGT	Exhaust Gas Temperature.
EOC	Engine Operational Cost
FSN	Filter Smoke Number.

GHG	Greenhouse Gas
HRR	Heat Release Rate.
HC	Hydrocarbons.
HD	Heavy Duty.
IMEP	Indicated Mean Effective Pressure.
IVO	Intake Valve Opening.
IVC	Intake Valve Closing
ISSoot	Net Indicated Specific Emissions of Soot.
ISNOx	Net Indicated Specific Emissions of NOx.
ISCO	Net Indicated Specific Emissions of CO.
ISHC	Net Indicated Specific Emissions of Unburned HC.
LIVC	Late Intake Valve Closing.
MFB	Mass Fraction Burnt
MAP	Manifold Air Pressure
NOx	Nitrogen Oxides.
NIE	Net Indicated Efficiency
$\mathbf{O_2}$	Oxygen
$\mathbf{P_{int}}$	Intake Pressure.
$\mathbf{P_{max}}$	Peak In-cylinder Pressure
PRR	Pressure Rise Rate
SCR	Selective Catalytic Reduction.
SOI	Start of Injection.
SOC	Start of Combustion.
TDC	Firing Top Dead Centre.
VVA	Variable Valve Actuation.
WHSC	World Harmonized Stationary Cycle.

References

1. Gravel, R., “Freight Mobility and SuperTruck,” 2016.
2. Dec, J.E., “A Conceptual Model of DI Diesel Combustion Based on Laser-Sheet Imaging*,” 1997, doi:10.4271/970873.
3. Rissman, B.J. and March, H.K., “Advanced Diesel Internal Combustion Engines,” (March):1–14, 2013.

4. Nations, U., “UNECE Regulation 49,” (March 1958), 2013.

5. Johnson, T. V., “Review of Vehicular Emissions Trends,” *SAE Int. J. Engines* 8(3), 2015, doi:10.4271/2015-01-0993.

6. Görsmann, C., “Improving air quality while reducing the emission of greenhouse gases,” *Johnson Matthey Technol. Rev.* 59(2):139–151, 2015, doi:10.1595/205651315X687524.

7. Cloudt, R., Baert, R., Willems, F., and Vergouwe, M., “SCR-only concept for heavy-duty Euro-VI applications,” *MTZ, Mot. Zeitschrift* 70(9):58–63, 2009, doi:10.1007/BF03226980.

8. Yao, M., Zhang, Q., Liu, H., Zheng, Z., Zhang, P., Lin, Z., Lin, T., and Shen, J., “Diesel Engine Combustion Control: Medium or Heavy EGR?,” *SAE Tech. Pap.* 1125–2010, 2010, doi:10.4271/2010-01-1125.

9. Liu, J., Wang, H., Zheng, Z., Zou, Z., and Yao, M., “Effects of Different Turbocharging Systems on Performance in a HD Diesel Engine with Different Emission Control Technical Routes,” *SAE Tech. Pap.*, 2016, doi:10.4271/2016-01-2185.

10. Vressner, A., Gabrielsson, P., Gekas, I., and Senar, E., “Meeting the EURO VI NOx Emission Legislation using a EURO IV Base Engine and a SCR / ASC / DOC / DPF Configuration in the World Harmonized Transient Cycle,” *Sae Pap. 2010-01-1216*, 2010, doi:10.4271/2010-01-1216.

11. Cloudt, R., Willems, F., and Heijden, P. van der, “Cost and Fuel Efficient SCR-only Solution for Post-2010 HD Emission Standards,” *SAE Int. J. Fuels Lubr.* 2(1):399–406, 2009, doi:10.4271/2009-01-0915.

12. Cavina, N., Mancini, G., Corti, E., Moro, D., Cesare, M. De, and Stola, F., “Thermal Management Strategies for SCR After Treatment Systems,” *SAE Int.*, 2013, doi:10.4271/2013-24-0153.

13. Baert, R.S.G., Beckman, D.E., and Veen, a, “SAE TECHNICAL Efficient EGR Technology for Future HD Diesel Engine Emission Targets,” *SAE Tech. Pap.* 1(0837):1–13, 1999, doi:10.4271/1999-01-0837.

14. Morgan, R., Banks, A., Auld, A., and Heikal, M., “The Benefits of High Injection Pressure on Future Heavy Duty Engine Performance,” (x), 2015, doi:10.4271/2015-24-2441.Copyright.

15. Buckendale, L.R., Stanton, D.W., and Stanton, D.W., “Systematic Development of Highly Efficient and Clean Engines to Meet Future Commercial Vehicle Greenhouse Gas Regulations,” *SAE Int.* 2013-01–2421, 2013, doi:10.4271/2013-01-2421.

16. Pedrozo, V.B., May, I., Guan, W., and Zhao, H., “High efficiency ethanol-diesel dual-fuel combustion: A comparison against conventional diesel combustion from low to full engine load,” *Fuel* 230(February):440–451, 2018, doi:10.1016/j.fuel.2018.05.034.

17. Charlton, S., Dollmeyer, T., and Grana, T., “Meeting the US Heavy-Duty EPA 2010 Standards and Providing Increased Value for the Customer,” *SAE Int. J. Commer. Veh.* 3(1):101–110, 2010, doi:10.4271/2010-01-1934.

18. Dallmann, T. and Menon, A., “Technology Pathways for Diesel Engines Used in Non-Road Vehicles and Equipment,” *ICCT White Pap.* (September), 2016.

19. Bruce Morey, “IAV brings variable valvetrains to heavy duty,” *SAE Int. United States*, 2017.

20. Imperato, M., Antila, E., Sarjovaara, T., Kaario, O., Larmi, M., Kallio, I., and Isaksson, S., “NOx Reduction in a Medium-Speed Single-Cylinder Diesel Engine using Miller Cycle with Very Advanced Valve Timing,” *SAE Tech. Pap.* 4970, 2009, doi:10.4271/2009-24-0112.

21. Rinaldini, C.A., Mattarelli, E., and Golovitchev, V.I., “Potential of the Miller cycle on a HSDI diesel automotive engine,” *Appl. Energy* 112(x):102–119, 2013,

doi:10.1016/j.apenergy.2013.05.056.

22. Gonca, G., Sahin, B., Parlak, A., Ayhan, V., Cesur, I., and Koksal, S., "Application of the Miller cycle and turbo charging into a diesel engine to improve performance and decrease NO emissions," *Energy* 93:795–800, 2015, doi:10.1016/j.energy.2015.08.032.

23. Benajes, J., Serrano, J.R., Molina, S., and Novella, R., "Potential of Atkinson cycle combined with EGR for pollutant control in a HD diesel engine," *Energy Convers. Manag.* 50(1):174–183, 2009, doi:10.1016/j.enconman.2008.08.034.

24. Guan, W., Pedrozo, V., Zhao, H., Ban, Z., and Lin, T., "Investigation of EGR and Miller Cycle for NOx Emissions and Exhaust Temperature Control of a Heavy-Duty Diesel Engine," *SAE Tech. Pap.*, 2017, doi:10.4271/2017-01-2227.

25. Kovács, D. and Eilts, P., "Potentials of the Miller Cycle on HD Diesel Engines Regarding Performance Increase and Reduction of Emissions," *SAE Tech. Pap. 2015-24-2440* (X), 2015, doi:10.4271/2015-24-2440.Copyright.

26. Zhang, Y., Wang, Z., Bai, H., Guo, C., and Li, Y., "The Reduction of Mechanical and Thermal Loads in a High- Speed HD Diesel Engine Using Miller Cycle with Late Intake Valve Closing," *SAE Tech. Pap.*, 2017, doi:10.4271/2017-01-0637.

27. Benajes, J., Molina, S., Martín, J., and Novella, R., "Effect of advancing the closing angle of the intake valves on diffusion-controlled combustion in a HD diesel engine," *Appl. Therm. Eng.* 29(10):1947–1954, 2009, doi:10.1016/j.applthermaleng.2008.09.014.

28. Guan, W., Pedrozo, V., Zhao, H., Ban, Z., and Lin, T., "Exploring the NOx Reduction Potential of Miller Cycle and EGR on a HD Diesel Engine Operating at Full Load," *SAE Tech. Pap.* 2018-April:1–12, 2018, doi:10.4271/2018-01-0243.

29. Gehrke, S., Kovács, D., Eilts, P., Rempel, A., and Eckert, P., "Investigation of VVA-Based Exhaust Management Strategies by Means of a HD Single Cylinder Research Engine and Rapid Prototyping Systems," *SAE Tech. Pap.* 01(0587):47–61, 2013, doi:10.4271/2013-01-0587.

30. Ratzberger, R., Kraxner, T., Pramhas, J., Hadl, K., Eichlseder, H., and Buergler, L., "Evaluation of Valve Train Variability in Diesel Engines," *SAE Int. J. Engines* 8(5):2015-24–2532, 2015, doi:10.4271/2015-24-2532.

31. Garg, A., Magee, M., Ding, C., Roberts, L., Shaver, G., Koeberlein, E., Shute, R., Koeberlein, D., McCarthy, J., and Nielsen, D., "Fuel-efficient exhaust thermal management using cylinder throttling via intake valve closing timing modulation," *Proc. Inst. Mech. Eng. Part D J. Automob. Eng.* 230(4):470–478, 2016, doi:10.1177/0954407015586896.

32. Guan, W., Zhao, H., Ban, Z., and Lin, T., "Exploring alternative combustion control strategies for low-load exhaust gas temperature management of a heavy-duty diesel engine," *Int. J. Engine Res.* 146808741875558, 2018, doi:10.1177/1468087418755586.

33. Schwoerer, J., Kumar, K., Ruggiero, B., and Swanbon, B., "Lost-Motion VVA Systems for Enabling Next Generation Diesel Engine Efficiency and After-Treatment Optimization," *SAE Tech. Pap.* 01(1189), 2010, doi:10.4271/2010-01-1189.

34. AVL., "AVL 415SE Smoke Meter," *Prod. Guid. Graz, Austria;*, 2013.

35. Regulation No 49 – uniform provisions concerning the measures to be taken against the emission of gaseous and particulate pollutants from compression-ignition engines and positive ignition engines for use in vehicles. Off J Eur Union, 2013.

36. Heywood J.B, "Internal Combustion Engine Fundamentals," ISBN 007028637X, 1988.

37. Zhao, H., "HCCI and CAI engines for the automotive industry," ISBN 9781855737426, 2007.

38. Hanson, R., Ickes, A., and Wallner, T., “Comparison of RCCI Operation with and without EGR over the Full Operating Map of a Heavy-Duty Diesel Engine,” *SAE Tech. Pap.* (x), 2016, doi:10.4271/2016-01-0794.

39. Johnson, T. V, “Diesel Emissions in Review,” *SAE Int. J. Engines* 4(1):143–157, 2011, doi:10.4271/2011-01-0304.

40. Pedrozo, V.B., May, I., and Zhao, H., “Exploring the mid-load potential of ethanol-diesel dual-fuel combustion with and without EGR,” *Appl. Energy* 193:263–275, 2017, doi:10.1016/j.apenergy.2017.02.043.

41. Ickes, A., Hanson, R., and Wallner, T., “Impact of Effective Compression Ratio on Gasoline-Diesel Dual-Fuel Combustion in a Heavy-Duty Engine Using Variable Valve Actuation,” 2015.

42. Modiyani, R., Kocher, L., Alstine, D.G. Van, Koeberlein, E., Stricker, K., Meckl, P., and Shaver, G., “Effect of intake valve closure modulation on effective compression ratio and gas exchange in turbocharged multi-cylinder engines utilizing EGR,” *Int. J. Engine Res.* 12(6):617–631, 2011, doi:10.1177/1468087411415180.

43. Pedrozo, V.B. and Zhao, H., “Improvement in high load ethanol-diesel dual-fuel combustion by Miller cycle and charge air cooling,” *Appl. Energy* 210(March 2017):138–151, 2018, doi:10.1016/j.apenergy.2017.10.092.

44. Stricker, K., Kocher, L., Koeberlein, E., Alstine, D. Van, and Shaver, G.M., “Estimation of effective compression ratio for engines utilizing flexible intake valve actuation,” *Proc. Inst. Mech. Eng. Part D J. Automob. Eng.* 226(8):1001–1015, 2012, doi:10.1177/0954407012438024.

45. Kawano, D., Suzuki, H., Ishii, H., Goto, Y., Odaka, M., Murata, Y., Kusaka, J., and Daisho, Y., “Ignition and Combustion Control of Diesel HCCI,” *Sae Tech. Pap. Ser.*, 2005, doi:10.4271/2005-01-2132.

46. Gehrke, S., Kovács, D., Eilts, P., Rempel, A., and Eckert, P., “Investigation of VVA-Based Exhaust Management Strategies by Means of a HD Single Cylinder Research Engine and Rapid Prototyping Systems,” *SAE Tech. Pap.* 01(0587):47–61, 2013, doi:10.4271/2013-01-0587.

47. Chi, J.N., “Control Challenges for Optimal NOx Conversion Efficiency from SCR Aftertreatment Systems,” *SAE Tech. Pap.*, 2009, doi:10.4271/2009-01-0905.

Appendix A. Test cell measurement devices

Variable	Device	Manufacturer	Measurement range	Linearity/Accuracy
Speed	AG 150 Dynamometer	Froude Hofmann	0-8000 rpm	± 1 rpm
Torque	AG 150 Dynamometer	Froude Hofmann	0-500 Nm	± 0.25% of FS
Diesel flow rate (supply)	Proline promass 83A DN01	Endress+Hauser	0-20 kg/h	± 0.10% of reading
Diesel flow rate (return)	Proline promass 83A DN02	Endress+Hauser	0-100 kg/h	± 0.10% of reading
Intake air mass flow rate	Proline t-mass 65F	Endress+Hauser	0-910 kg/h	± 1.5% of reading
In-cylinder pressure	Piezoelectric pressure sensor Type 6125C	Kistler	0-300 bar	≤ ± 0.4% of FS
Intake and exhaust pressures	Piezoresistive pressure sensor Type 4049A	Kistler	0-10 bar	≤ ± 0.5% of FS
Oil pressure	Pressure transducer UNIK 5000	GE	0-10 bar	< ± 0.2% FS
Temperature	Thermocouple K Type	RS	233-1473K	≤ ± 2.5 K
Intake valve lift	S-DVRT-24 Displacement Sensor	LORD MicroStrain	0-24 mm	± 1.0% of reading using straight line
Smoke number	415SE	AVL	0-10 FSN	-
Fuel injector current signal	Current Probe PR30	LEM	0-20A	± 2 mA